Making Things Last Longer®
118 Lincoln St.
Lunenburg, Nova Scotia B0J 2C0
(902) 329-5466
www.deepcryogenics.com

Deep Cryogenic Treatment of Cast Iron

Three types of cast iron (G2 gray, 65-45 ductile and 80-55) were DC-treated and tested to observe principal changes in microstructure. All samples were prepared from round bar (Fig. 1), ground 120-1,200 on a Pace twin platen grinder, polished to 1µm with diamond suspension and etched using 2% nital. Micrographs were taken using an Olympus BX-53 microscope and apochromatic lenses in both baseline and DCT state. Pre-etch micrographs were used for examination and characterization of graphite constituents and etched micrographs were used to examine ferrite and perlite changes. Deep cryogenic treatment was performed by DCI in Lunenburg, Canada with a CP-200 cryogenic tank in a dry nitrogen gas environment (Fig. 2).

Materials Plus image analysis software (MP) was used to analyze size and distribution of the graphite while ImageJ software was employed to segment and observe sample nodularity.

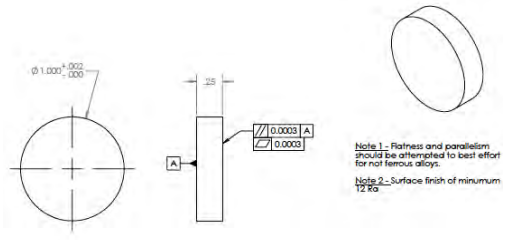

Figure 1: DCI's standardized lab coupons

Figure 2: CP-200 tank at DCI

1 G2 Gray Cast Iron

1.1 Microstructure

Quantification of the size and distribution of flake graphite (size range: 1-8) and type of graphite flake (A,B,C,D and E) were measured in accordance with ASTM 247-67.

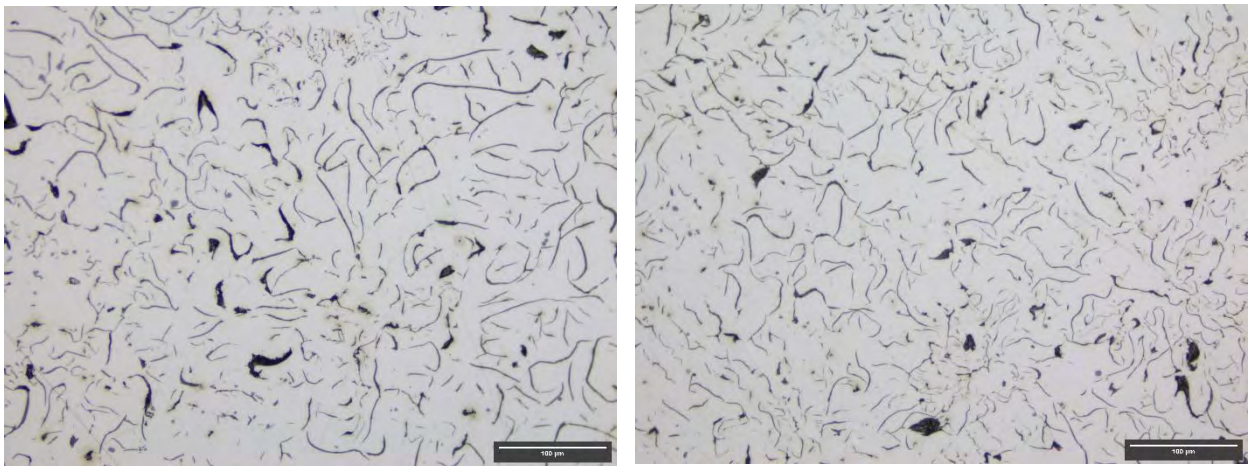

Figure 3: Micrographs of G2 cast iron as polished, baseline (left) and DCT (right); 200x mag

Comparing the two states (baseline vs. DCT) measured using MP software shows that DCT increased graphite flake quantity in the 4,5 and 6 size range while reducing quantities in the

1 and 2 size range (Fig. 4). Furthermore, the software measured a reduction in Type A flake and an increase of Type D and E flake in the DCT micrograph vs. baseline (Fig. 5).

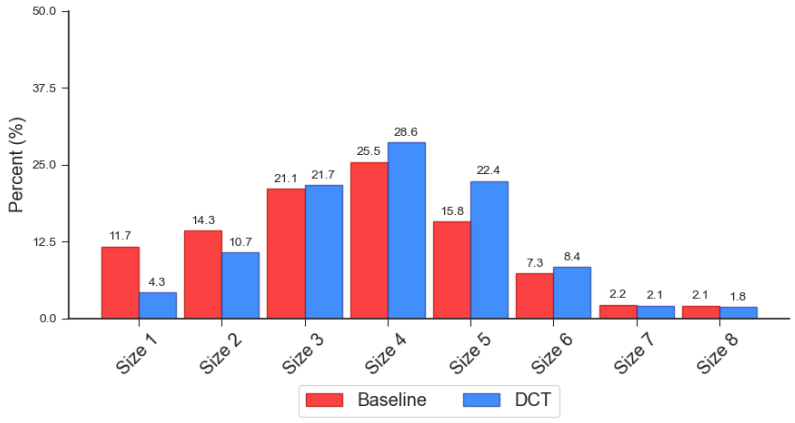

Figure 4: Size distribution of G2 cast iron flakes (200x mag)

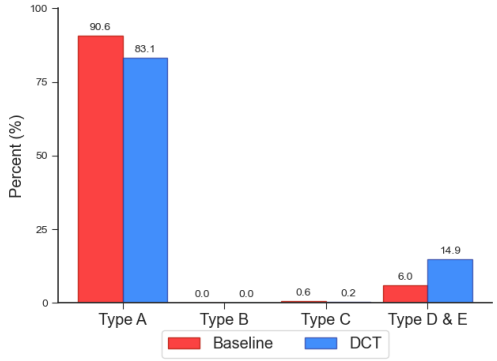

Figure 5: Flake type distribution of G2 cast iron (200x mag)

The micrographs in Fig. 6 were segmented to measure the amount of graphite in each sample. Micrographs taken at higher magnification shown in Fig. 7 resolve the fine pearlitic bulk structure not clearly visible in Fig. 6. Fig. 7 left also displays spherical and angular inclusions measuring roughly 14μm^2 and 3μm^2 respectively (red arrows) and are likely manganese sulphides. Manganese sulphides can restrict graphitisation but have little influence on the material's castability and use properties of commercial cast irons [1].

Both the baseline and DCT micrographs underwent the identical image processing techniques to obtain quantification of the graphite. This process primarily included use of ImageJ software and its various modules. The segmented graphite, shown in Fig. 8, illustrate that the DCT sample displayed graphite flakes that are more randomly oriented, smaller in size and evenly distributed than the baseline sample [1]. Increased thermal conductivity and wear resistance are aligned with such improvements observed in the graphite flakes in the DCT gray iron [2].

Upon visual inspection of the non-etched micrographs presented in Fig. 3, this tendency is repeated in the DCT sample displaying smaller, more evenly dispersed graphite flakes. The DCT sample also displayed a higher total graphite content, from 11.25% to 12.23%.

118 Lincoln St.
Lunenburg, Nova Scotia B0J 2C0
(902) 329-5466
www.deepcryogenics.com

The high magnification micrographs in Fig. 7 correspond to the findings of Thornton [2] with a more even distribution into the graphite flakes post-DCT. A similar 'thinning' and 'roughness' is observed after DCT, along with fewer MnS inclusions than found in baseline.

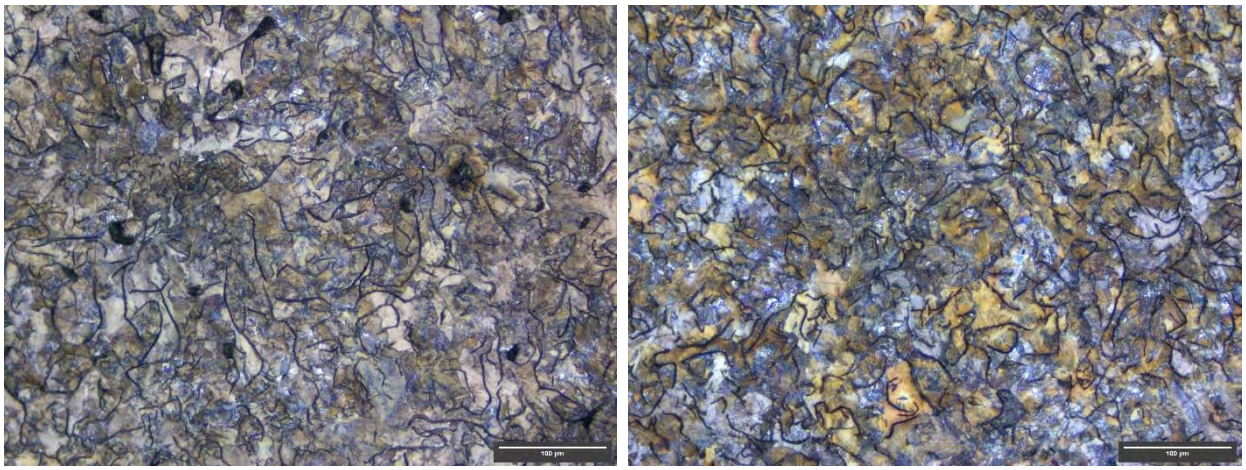

Figure 6: Micrographs of G2 cast iron etched with 2% Nital, baseline (left) and DCT (right); 200x mag

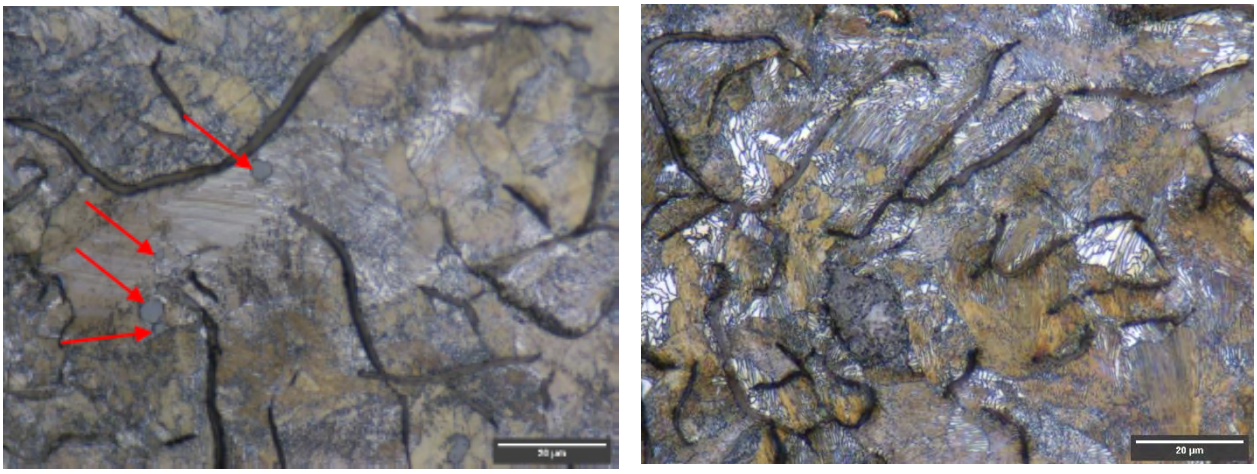

Figure 7: Micrographs of G2 cast iron etched with 2% Nital, baseline (left) and DCT (right); 1000x mag

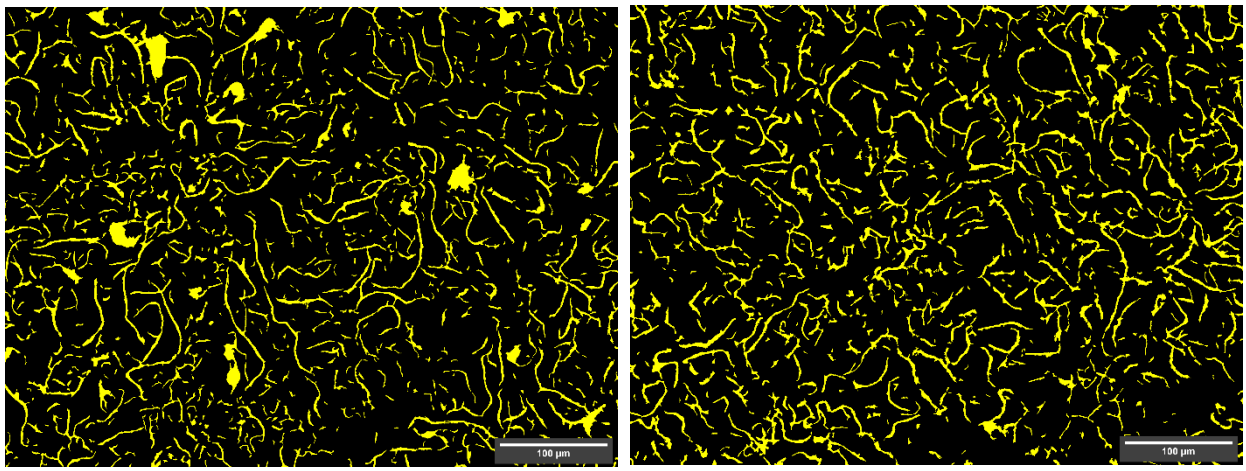

Figure 8: Segmentation overlay from Figure 6, baseline (left) and DCT (right), graphite in yellow; 200x mag

1.2 Hardness

The hardness of the G2 cast iron was measured before and after DCT using a Microstar DigiRock DR3 calibrated digital hardness tester with the results displayed in Fig. 9. The DCT had no noticeable effect on the hardness of the material. This corresponds with studies conducted on similar gray iron (G10 cast iron) by Thornton [2], where no significant change in hardness for G10 cast iron was found due to DCT.
Fig. 9 shows the bimodal effect of DCT on hardness, as compared to DCT 80-55 cast iron.

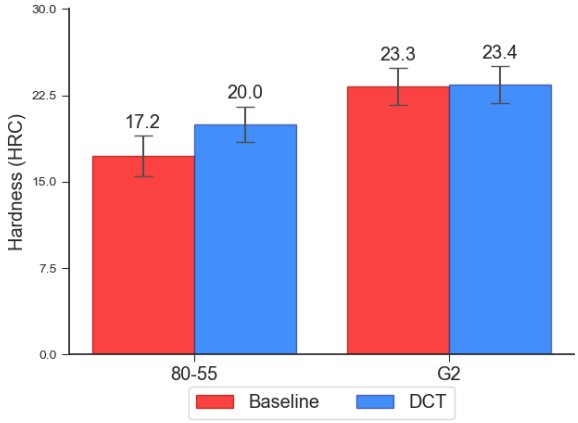

Figure 9: Hardness results for 80-55 and G2 cast iron

1.3 SWLI Surface Finish

Surface finish measurements were taken using a Filmetrics Scanning White Light Interferometer (SWLI) on an 'as-cut' surface, prepared with a Kalamazoo K-12 metallurgical sectioning saw. Each sample was scanned three times in nine different locations. Each location was examined, and any anomalies in the readings excluded from the dataset.

Four areal surface measurements were examined to determine if there was any effect on the surface of the material due to DCT: average height, arithmetic mean height (Sa), root mean square height (Sq), and core height (Sk). The measurements show that DCT does not affect the surface finish of these cast iron materials.

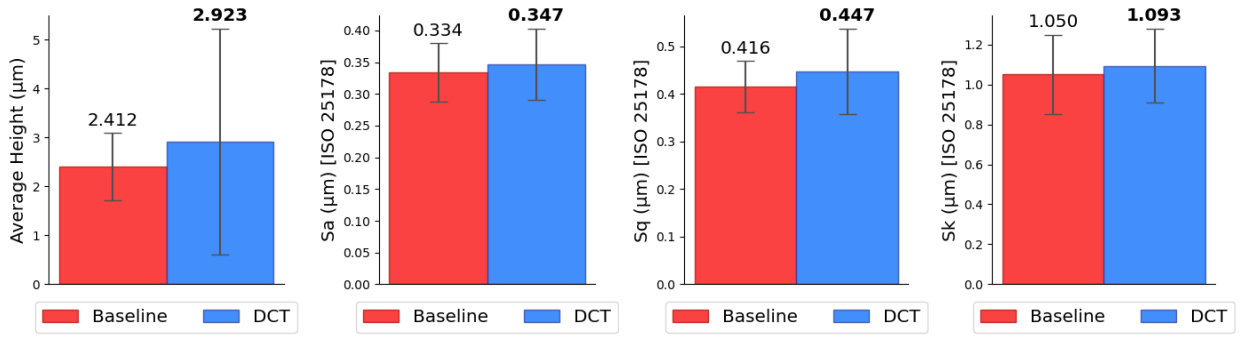

Figure 10: Surface finish measurements for Average height, Sa, Sq, and Sk for G2 cast iron

1.4 Ferrite and Martensite

Fig. 11 displays results measured with a Fischer Feritscope FMP30C and are the average of five measurements. The G2 results in Fig. 11 show a slight decrease in both ferrite and martensite content, similar to the results in 80-55 cast iron, while 65-45 ductile cast iron shows a significant increase in sampled ferrite and martensite content following DCT.

Note that the increased hardness of 80-55 from DCT (Fig. 9) is not inversely correlated or explainable by the reduction in martensite volume fraction observed in Fig. 11. Readily identifiable and predictable correlations between changes to phase, microstituents or hardness and DCT-attributed improvement to wear improvement, ultimate tensile/yield strength and surface finish post have yet to be established.

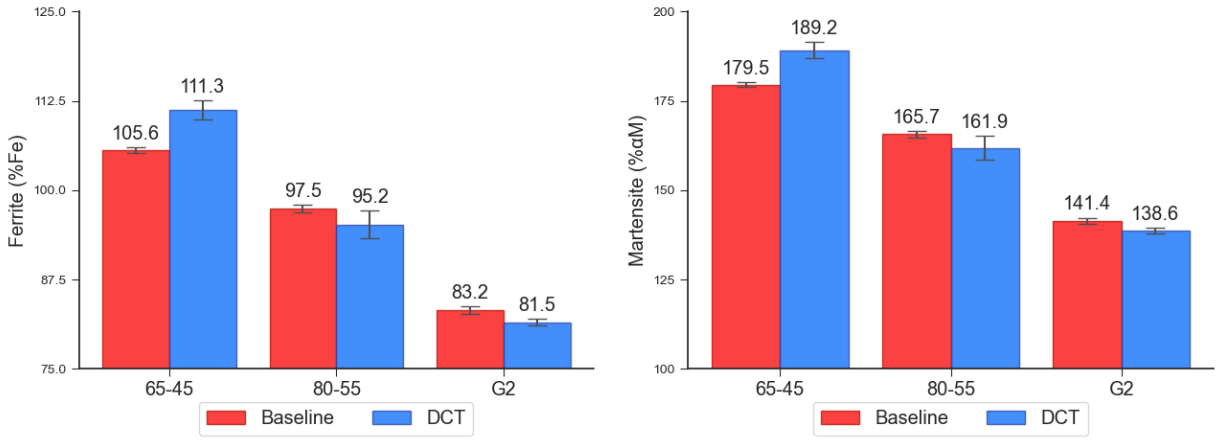

Figure 11: Ferrite (left) and martensite (right) measurements for 65-45, 80-55, and G2 cast irons

2 65-45-12 Ductile Cast Iron

2.1 Microstructure

Quantification of the size distribution of nodular graphite (size range: 1-8) and type of graphite flake (A,B,C,D and E) were measured by MR image analysis module.

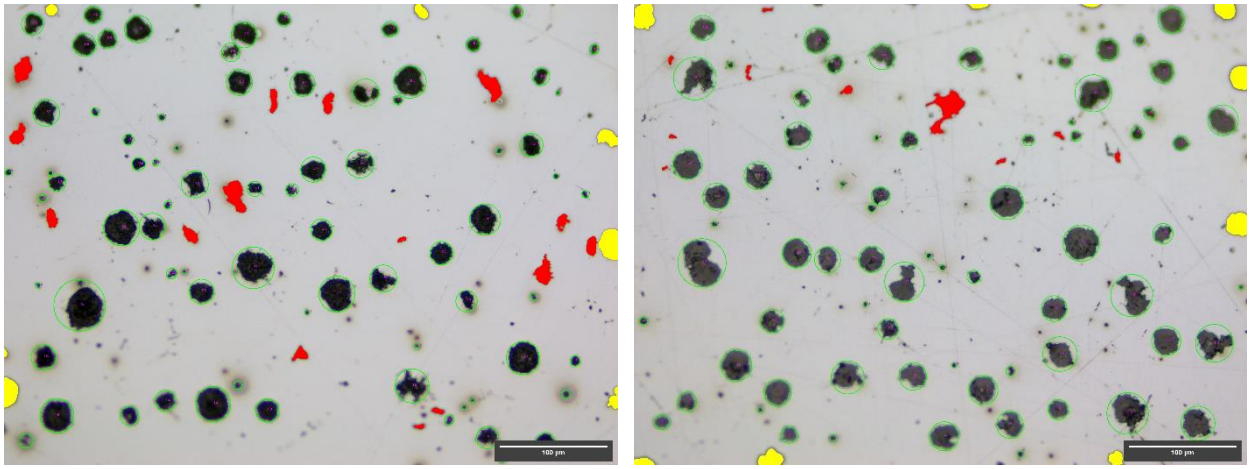

Figure 12: Micrographs of 65-45-12 cast iron, baseline (left) and DCT (right); 200x mag

Comparing the two states (baseline vs. DCT) using MR software shows that the DCT sample displayed only slight changes in the sizes of the graphite nodules (Fig. 13). Furthermore, the software measured no significant change in the type of graphite nodule (Fig. 14).

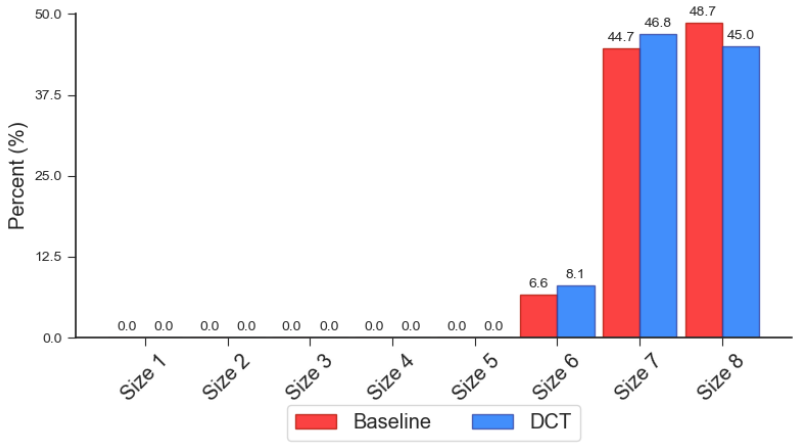

Figure 13: Size distribution of 65-45-12 cast iron nodules (200x mag)

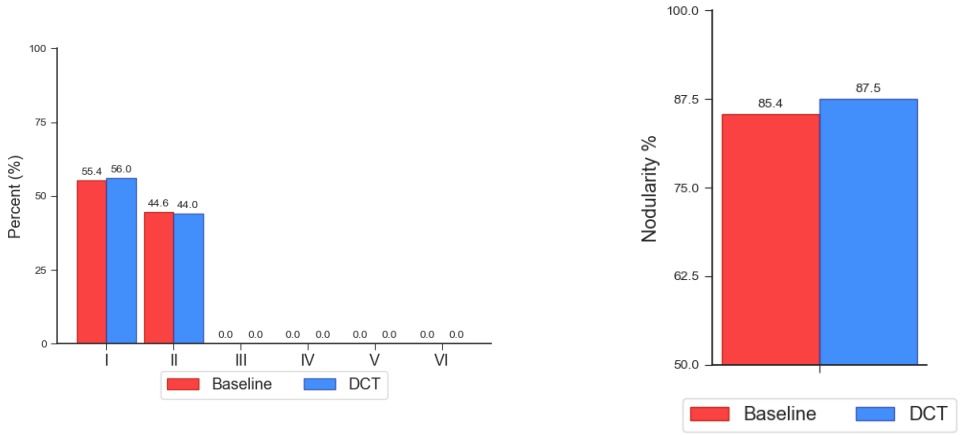

Figure 14: Nodule type distribution (left) and nodularity (right) of 65-45-12 cast iron (200x mag)

The micrographs in Fig. 15 were segmented to measure the amount of graphite and free ferrite in each sample. Both the baseline and DCT micrographs underwent the identical image processing techniques to obtain quantification of the graphite and free ferrite. This process primarily included use of ImageJ software and its various modules. The segmented graphite, shown in Fig. 16, illustrates that the graphite nodules are more evenly distributed.

The free ferrite (white in Fig. 15) was also segmented, allowing for amounts of each phase to be compared between the two states. The results are shown in Table 1. The measurements show that the DCT sample has less pearlite and more ferrite compared to the baseline micrograph. The graphite content of the DCT micrograph is slightly higher than that in the baseline.

	Ferrite	Graphite	Pearlite
Baseline	56.29%	10.27%	33.45%
DCT	61.43%	10.90%	27.66%

Table 1: Phase percentages from segmentation of micrographs in Figure 15

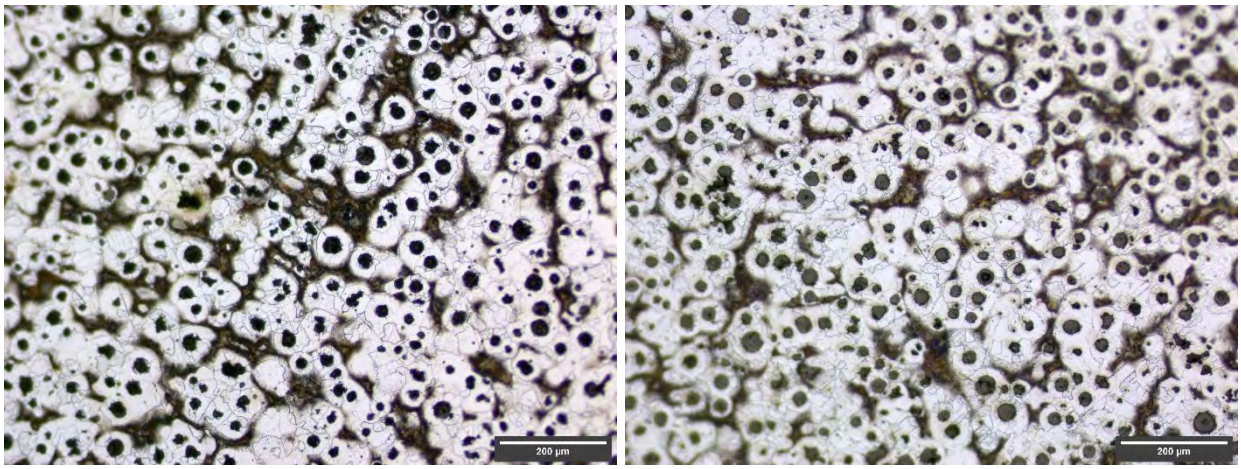

Figure 15: Micrographs of 65-45 cast iron etched with 2% Nital, baseline (left) and DCT (right); 100x mag

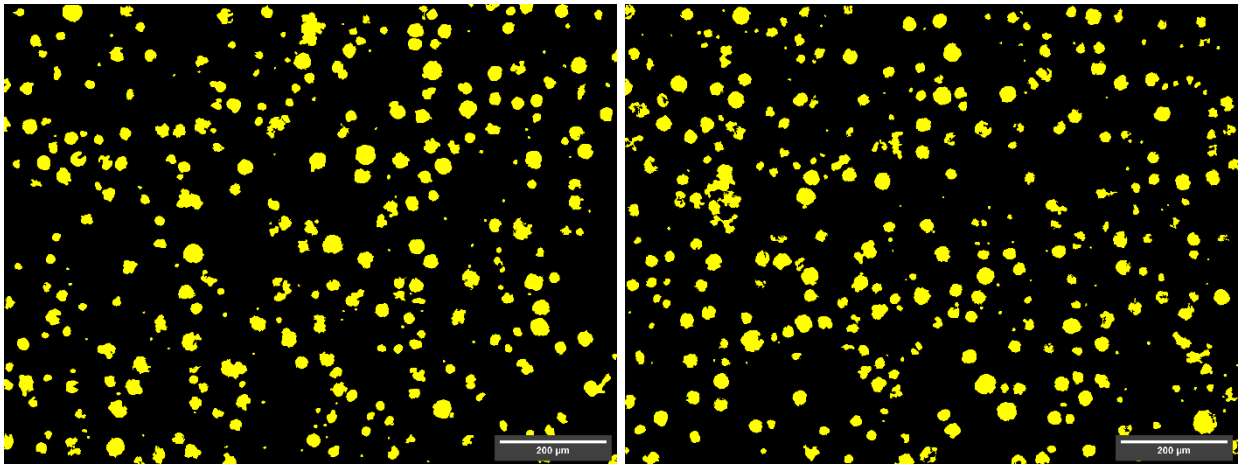

Figure 16: Segmentation overlay of micrographs; baseline (left) and DCT (right), graphite in yellow; 100x mag

2.2 Hardness

The hardness of the 65-45 cast iron was measured before and after DCT, with the results displayed in Fig. 17. The DCT treatment had no noticeable effect on the material hardness.

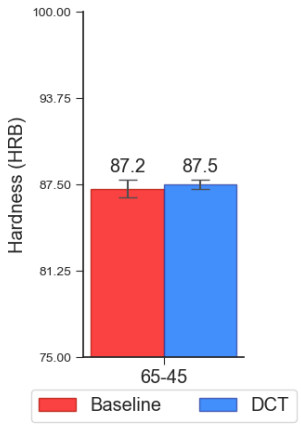

Figure 17: Hardness measurements for 65-45 cast iron

2.3 SWLI Surface Finish

The 65-45-12 material had surface measurements conducted using a SWLI on an 'as-cut' surface, which was sectioned using a metallurgical sectioning saw. Each sample was scanned three times in nine different locations and averaged as per the G2 procedure shown in Section 1.3 The measurements indicate that DCT does not affect the surface finish of 65-45.

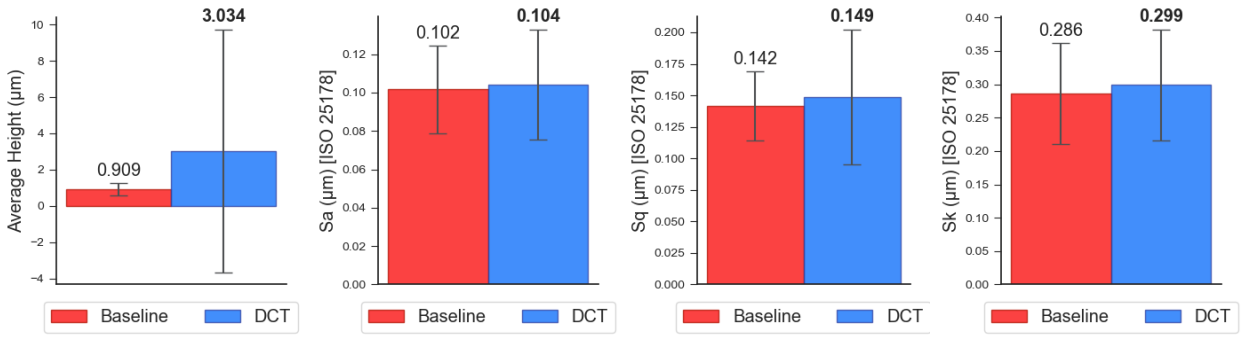

Figure 17: Surface finish measurements for Average height, Sa, Sq, and Sk for 65-45 cast iron

2.4 Ferrite and Martensite

The results for 65-45 in Fig 11 show a clear increase in ferrite and martensite volume fraction.

3 80-55 Ductile Cast Iron

3.1 Microstructure

Quantification of the size distribution of nodular graphite (size range: 1-8) and type of graphite flake (A,B,C,D and E) were measured by the MR software module.

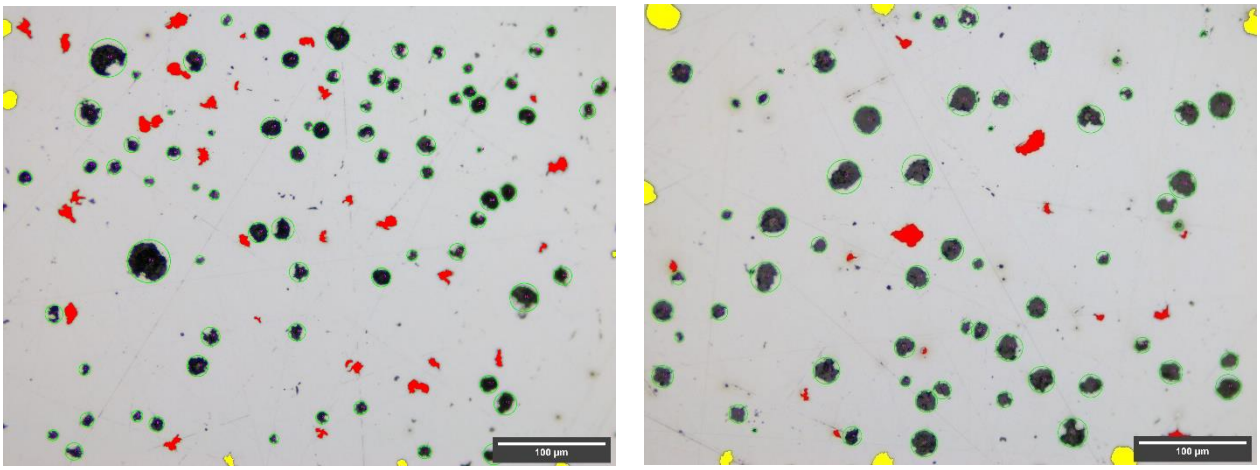

Figure 18: Micrographs of 80-55 cast iron, baseline (left) and DCT (right); 200x mag

Comparing the two states (baseline vs. DCT) using MR software shows that the DCT sample displayed only slight changes in the sizes of the graphite nodules (Fig. 19). Furthermore, the software measured no significant change in the type of graphite nodule (Fig. 20).

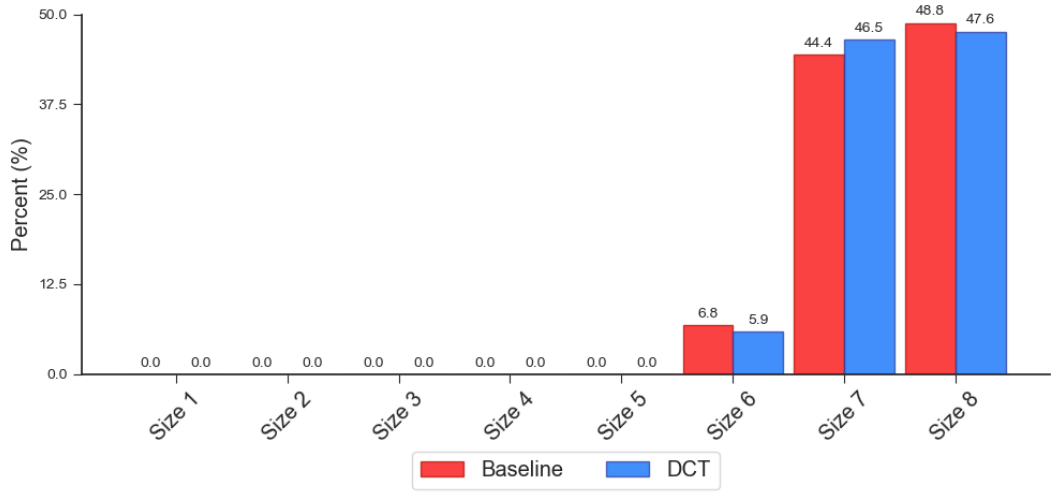

Figure 19: Size distribution of 80-55 cast iron nodules (200x mag)

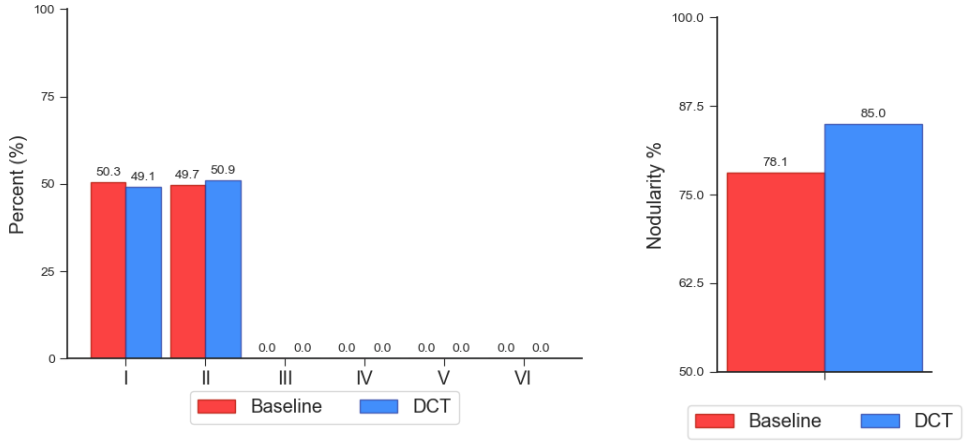

Figure 20: Nodule type distribution (left) and nodularity (right) of 80-55 cast iron (200x mag)

The micrographs in Fig. 21 were segmented to measure the amount of graphite and free ferrite in each sample. Both the baseline and DCT micrographs underwent the identical image processing techniques to obtain quantification of the graphite and free ferrite. This process primarily included use of ImageJ software and its various modules. The segmented graphite, shown in Fig. 22, illustrates that the graphite nodules are similarly distributed.

The free ferrite (white in Fig. 14) was also segmented, allowing for amounts of each phase to be compared between the two states. The results are shown in Table 2. The measurements show that the DCT sample has more pearlite and less ferrite compared to the baseline micrograph, albeit marginal. The graphite content of the DCT is slightly higher than baseline.

	Ferrite	Graphite	Pearlite
Baseline	33.18%	8.04%	58.78%
DCT	31.16%	8.58%	60.26%

Table 2: Phase percentages from segmentation of micrographs in Figure 14

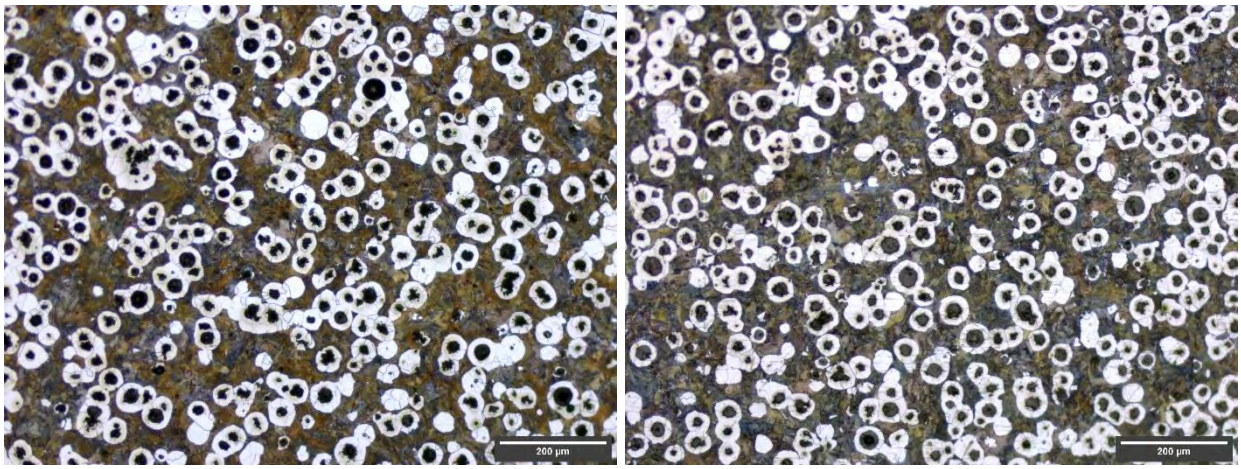

Figure 21: Micrographs of 80-55 cast iron etched with 2% Nital, baseline (left) and DCT (right); 100x mag

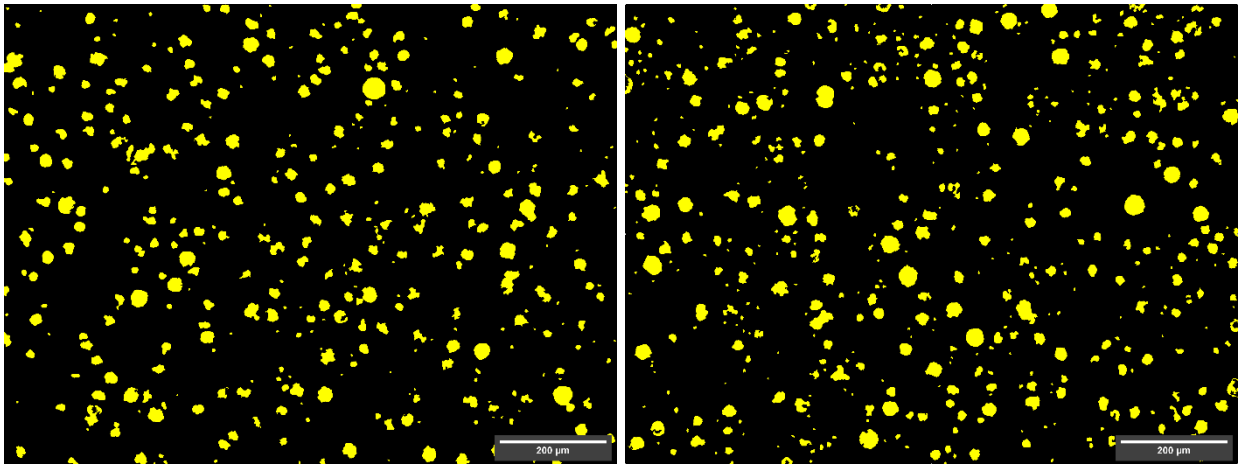

Figure 22: Segmentation of micrographs from Figure 21, baseline (left) and DCT (right), graphite in yellow; 100x mag

3.2 Hardness

The hardness of the 80-55 cast iron was measured before and after DCT, with the results displayed in Fig. 23. DCT increased the hardness of the material by just under 3Rc.

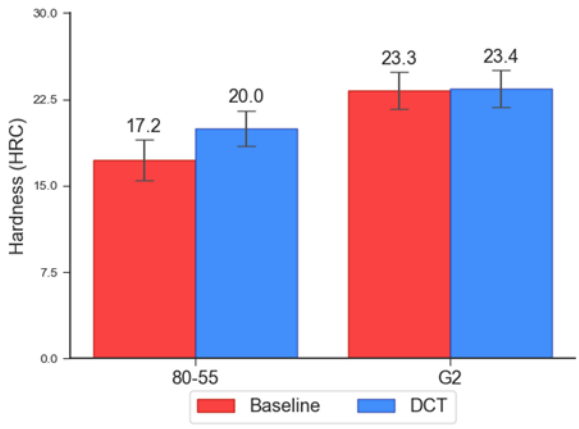

Figure 23: Hardness results for 80-55 and G2 cast iron

3.3 SWLI Surface Finish

The 80-55 cast iron had surface measurements conducted on it using a SWLI on an 'as-cut' surface, which was sectioned using a metallurgical sectioning saw. Each sample was scanned three times in nine different locations and averaged.

Four areal surface measurements were examined to determine if there was any effect on the surface of the material due to DCT: average height, arithmetic mean height (Sa), root mean square height (Sq), and core height (Sk). All the measurements indicated a decrease in each feature: however, further testing is needed as all results are within one standard deviation. The results for the measurements are shown in Fig. 24.

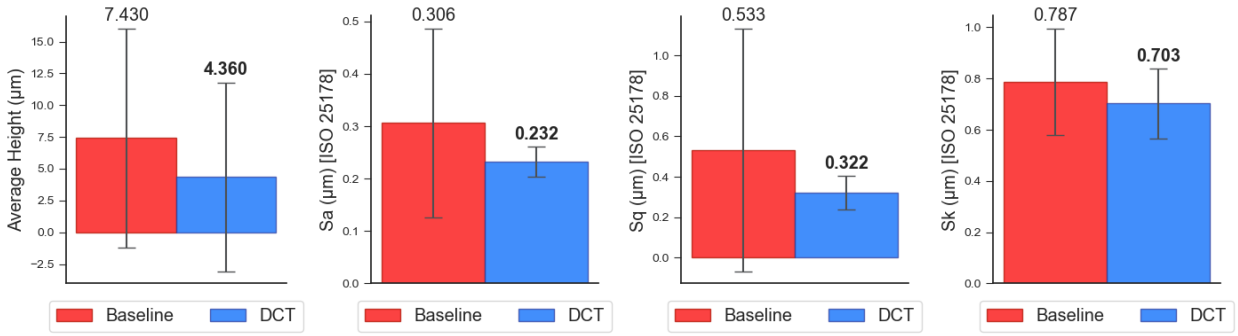

Figure 24: Surface finish measurements for Average height, Sa, Sq, and Sk for 80-55 cast iron

3.4 Ferrite and Martensite

The 80-55 measurements show a slight decrease in ferrite and martensite volume fractions.

4 References

[1] W. F. Smith, Structure and Properties of Engineering Alloys, McGraw-Hill, Inc, 1981.

[2] R. W. Thornton, T. Slatter and R. Lewis, *Investigating the effects of cryogenic processing on the wear performance and microstructure of engineering materials,* The University of Sheffield, 2014.

5 Summary

DCT improved the following cast iron properties:

5.1 Graphite

- Graphite content of the G2 gray iron increased 8.71%
- Morphology of the G2 gray iron became more evenly dispersed
- Graphite content of the 65-45-12 ductile iron increased 6.13%
- Graphite nodularity of the 65-45-12 ductile iron increased 2.46%
- Graphite content of the 80-55-06 ductile iron increased 6.72%
- Graphite nodularity of the 65-45-12 ductile iron increased 8.84%

5.2 Pearlite and Ferrite in the Ductile Cast Iron

- Ferrite content of the 65-45-12 ductile iron increased 9.13%
- Pearlite content of the 65-45-12 ductile iron decreased 17.31%
- Ferrite content of the 80-55-06 ductile iron decreased 6.01%
- Pearlite content of the 80-55-06 ductile iron increased 2.52%

5.3 Inclusions in the Gray Iron

- Visual inspection revealed reduction in MnS inclusions

5.4 Hardness Measurements

- Hardness of the 80-55-06 ductile iron increased by approximately 3Rc

6 Conclusion

While the sample size is small, the testing for this paper was conducted to probe at which areas require heavier investigation in terms of effects on industrial cast irons due to deep cryogenic treatments. The results discussed in this paper are intended to highlight possible areas in which DCT can be beneficial to the performance of industrial use cast irons.

Notable findings were:

- In all samples the graphite content increased
- In the G2 gray iron the graphite was more dispersed
- In both ductile irons the nodularity increased
- MnS inclusions were reduced in the G2 gray iron sample
- 80-55-02 ductile iron showed an increase in hardness

Highly significant observations of wear improvement in ductile, austempered, gray and white cast iron have been noted in more than a dozen academic studies employing destructive test equipment such as pin-on-disc, pin-on-plate, brake rotor tests and slurry erosion tests. The microstructure changes noted in this paper should be compared with such mechanical tests noted above in order to correlate lab test observations with applied field test data.